A Letters Journal Exploring the Frontiers of Physics

August 2011

EPL, **95** (2011) 36002
doi: 10.1209/0295-5075/95/36002

www.epljournal.org

Attraction between like-charge surfaces in polar mixtures

S. Samin and Y. Tsori[(a)]

Department of Chemical Engineering and The Ilse Katz Institute for Nanoscale Science and Technology, Ben-Gurion University of the Negev - 84105 Beer-Sheva, Israel

received 26 April 2011; accepted in final form 16 June 2011
published online 15 July 2011

PACS 64.70.Ja – Liquid-liquid transitions
PACS 64.75.Xc – Phase separation and segregation in colloidal systems
PACS 64.75.Jk – Phase separation and segregation in nanoscale systems

Abstract – We examine the force between two charged surfaces immersed in aqueous mixtures having a coexistence curve. For a homogeneous water-poor phase, as the distance between the surfaces is decreased, a water-rich phase condenses at a distance D_t in the range 1–100 nm. At this distance the osmotic pressure can become negative leading to a long-range attraction between the surfaces. The osmotic pressure vanishes at a distance $D_e < D_t$, representing a very deep metastable or globally stable energetic state. We give analytical and numerical results for D_t and D_e on the Poisson-Boltzmann level.

The forces between charged objects in electrolyte solutions are of fundamental importance in biology and colloidal science. Within the Poisson-Boltzmann (PB) mean-field theory, in a single pure solvent, the interaction between symmetrically charged colloids is always repulsive [1]. Experiments, on the other hand, have shown that highly charged colloids can attract each other when multivalent ions are present. This discrepancy has been explained theoretically by counterion correlations [2], fluctuation-induced forces [3] and other non-electrostatic interactions [4]. More recently, the PB theory was generalized by strong coupling theory [5,6], which predicts an attraction for large values of the so-called coupling parameter [7,8].

In this letter we use the PB theory to show that strong attractive forces appear between similarly charged colloids in *mixtures*. In mixtures one must also take into account that the medium itself becomes inhomogeneous due to dielectrophoretic and solvation-related forces. The preferential solvation energy of ions in one of the solvents [1,9] is appreciable and can even be much larger than the thermal energy [10–12]. For a recent review on ion-specific solvation effects within the PB theory see [13]. Previous works on preferential solvation in binary mixtures looked at the phase behavior in the bulk [14,15], surface tension [16], and the interaction between surfaces but not in immiscible liquids [17]. As is shown below, in partially miscible mixtures, the behavior is qualitatively different and strong forces occur. In colloidal suspensions these forces can have an important role not studied before [18–22].

We consider two positively charged colloids in a mixture of polar solvents. The colloids are modeled as flat surfaces located at $z = \pm D/2$ and uniformly charged with a charge density $e\sigma$ per unit area, where e is the elementary charge. A small amount of monovalent ions and weakly charged surfaces are assumed and therefore the coupling parameter is small and the PB theory is applicable [6]. The partially miscible solvents have a coexistence curve below the mixture critical temperature T_c in the absence of ions. This coexistence curve is further modified by the presence of ions [15].

The grand potential density is given by [14,23]

$$\begin{aligned}\frac{\omega}{T} = {} & f_b(\phi) + \frac{C}{2}|\nabla\phi|^2 + \frac{1}{2T}\varepsilon(\phi)(\nabla\psi)^2 \\ & + n^+\left(\log(v_0 n^+) - 1\right) + n^-\left(\log(v_0 n^-) - 1\right) \\ & - (\Delta u^+ n^+ + \Delta u^- n^-)\phi - \lambda^+ n^+ - \lambda^- n^- - \mu\phi.\end{aligned} \tag{1}$$

Here the Boltzmann constant is set to unity, T is the thermal energy and C is a positive constant. ϕ is the volume fraction of water ($0 \leqslant \phi \leqslant 1$); far away from the surfaces the mixture is homogeneous and water-poor with composition $\phi_0 < 1/2$ and ion densities n_0. We use a regular solution form for the free energy of a binary mixture $v_0 f_b = \phi\log(\phi) + (1-\phi)\log(1-\phi) + \chi\phi(1-\phi)$ [24], where $\chi \sim 1/T$ is the Flory parameter and $v_0 = a^3$ is the molecular volume of both liquids. The third term in eq (1) is the

(a) E-mail: tsori@bgu.ac.il

electrostatic energy of the mixture, where ψ is the electrostatic potential. The mixture dielectric constant depends on the composition through a linear relation: $\varepsilon(\phi) = \varepsilon_c + (\varepsilon_w - \varepsilon_c)\phi$, where ε_c and ε_w are the pure cosolvent and water dielectric constants, respectively. The second line of eq. (1) is the ideal gas entropy of point-like ions, where n^+ and n^- are the positive and negative ion density, respectively. The first term on the third line is the bilinear solubility interaction of the ions and the solvent: the parameters Δu^+ and Δu^- measure the affinity of the positive and negative ions toward the water environment, respectively. We use the common case where both ions are hydrophilic and assume the symmetric interaction $\Delta u^+ = \Delta u^- = \Delta u > 0$. Lastly, $\lambda^\pm$ and μ are the Lagrange multipliers (chemical potentials) of the positive and negative ions and water composition, respectively.

The ion densities obey the Boltzmann distribution

$$n^\pm = v_0^{-1} \mathrm{e}^{\lambda^\pm} \mathrm{e}^{\mp e\psi/T + \Delta u \phi}. \tag{2}$$

In a salt reservoir we have $\lambda^\pm = \log(v_0 n_0) - \Delta u \phi_0$. Alternatively, when the mixture contains only negative counterions, λ^- is determined self-consistently by charge conservation: $\int n^- \mathrm{d}z = 2\sigma$.

The electrostatic potential is determined by the Poisson equation

$$\nabla \cdot (\varepsilon(\phi) \nabla \psi) = -e(n^+ - n^-) \tag{3}$$

supplemented by the boundary condition on the surfaces $-\mathbf{n} \cdot \nabla\psi(\pm D/2) = e\sigma/\varepsilon(\phi)$, where $\mathbf{n}$ is the outward unit normal to the surface. Finally, the Euler-Lagrange equation for ϕ reads

$$C\nabla^2\phi = \frac{\partial f_b}{\partial \phi} - \frac{1}{2T}\frac{\mathrm{d}\varepsilon}{\mathrm{d}\phi}(\nabla\psi)^2 - \Delta u(n^+ + n^-) - \mu. \tag{4}$$

In order to isolate electrostatic effects from the regular wetting-like behavior, we assume zero short-range chemical or long-range van der Waals interactions with the surfaces, leading to the boundary condition $\mathbf{n} \cdot \nabla\phi(z = \pm D/2) = 0$.

The net force exerted on the surfaces by the liquid is given by the osmotic pressure $\Pi = P_{zz} - P_b$, where P_b is the bulk pressure: $P_b/T = \phi_0 \partial f_b(\phi_0)/\partial\phi - f_b(\phi_0) + 2n_0(1 - \Delta u \phi_0)$. $-P_{zz}$ is the zz component of the Maxwell stress tensor [17,25]:

$$\frac{P_{zz}}{T} = \frac{C}{2}\left(\frac{\mathrm{d}\phi}{\mathrm{d}z}\right)^2 - C\phi\frac{\mathrm{d}^2\phi}{\mathrm{d}z^2} + \phi\frac{\partial f_b}{\partial\phi} - f_b + (1 - \Delta u\phi)(n^+ + n^-) - \frac{1}{2T}\left(\phi\frac{\mathrm{d}\varepsilon}{\mathrm{d}\phi} + \varepsilon\right)\left(\frac{\mathrm{d}\psi}{\mathrm{d}z}\right)^2; \tag{5}$$

P_{zz} is independent of z and can be calculated at the midplane ($z = 0$) where by symmetry $\mathrm{d}\phi/\mathrm{d}z = \mathrm{d}\psi/\mathrm{d}z = 0$. Multiplying eq. (4) by ϕ and inserting into eq. (5) we obtain

$$\Pi = Tn_m - T\omega_b(\phi_m) - P_b, \tag{6}$$

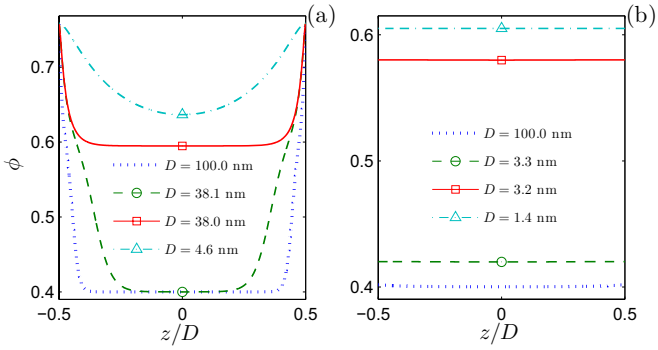

Fig. 1: (Colour on-line) (a) Composition profiles $\phi(z)$ in the strong screening limit for $D < D_t$ (dotted line), just before and after D_t (dashed and solid lines) and at D_e (dash-dot line). Here $n_0 = 0.1$ M, $\Delta u = 2$ and $\sigma = 1\,\mathrm{nm}^{-2}$. (b) The same in the ideal gas regime with no salt, $\Delta u = 11$ and $\sigma = 0.01\,\mathrm{nm}^{-2}$. Here and, unless stated otherwise, in all other figures we took for the mixture $\phi_0 = 0.4$, $T/T_c = 0.9915$ and $C = \chi/a$ [24]. As an approximation of a water–1-butanol mixture we used $T_c = 398$ K, $v_0 = 3 \times 10^{-29}\,\mathrm{m}^3$, $\varepsilon_c = 17.8$ and $\varepsilon_w = 80$.

where $\omega_b = f_b - \mu\phi$ and ϕ_m and n_m are the composition and total ion density at the midplane, respectively.

In aqueous mixtures, water is drawn towards the walls by field gradients (dielectrophoretic) and solvent-induced (electrophoretic) forces [17,23,26]. These forces are interdependent as is evident from eqs. (3) and (4). From the solution of the governing equations we find two possible scenarios, distinguished according to the composition profiles at infinite separation. In the first scenario, when the surfaces are far apart, $\phi(z)$ near each surface is composed of three layers: a thin water-rich layer ($\phi > 1/2$) of width t at the surfaces, a second layer with width of the bulk correlation length ξ adjacent to it, where the composition $\phi \gtrsim \phi_0$ decays to the bulk value, and a third "bulk" layer where $\phi \approx \phi_0$ [23].

As the surface separation decreases down to $D = D_t$, the general features of this profile do not change. In particular, only the width of the $\phi \approx \phi_0$ region changes if screening is strong, that is, when $l_D \ll D$ where $l_D \sim n_0^{-1/2}$ is the Debye length calculated at $\varepsilon = \varepsilon(\phi_0)$. The dashed curve in fig. 1(a) shows $\phi(z)$ just before D_t for this case.

In the second scenario, dielectrophoretic and solvation forces are not strong enough and at large surface separations ϕ is always close to the bulk value ϕ_0. As D decreases from infinity the water composition between the surfaces increases continuously. In particular, in the ideal gas regime, defined by $b \gg D$, where $b \propto \sigma^{-1}$ is the Gouy-Chapman length, $\phi(z)$ is nearly uniform. Figure 1(b) shows such profiles for a mixture containing only counterions. Here, the ion profile $n(z)$ and electric field are nearly uniform leading to small composition gradients.

In both scenarios, when $D < D_t$ the whole space between the surfaces becomes rich in water (see the solid curves in fig. 1). The transition occurs at a distance in the range $D_t = 1$–100 nm depending on the parameter values,

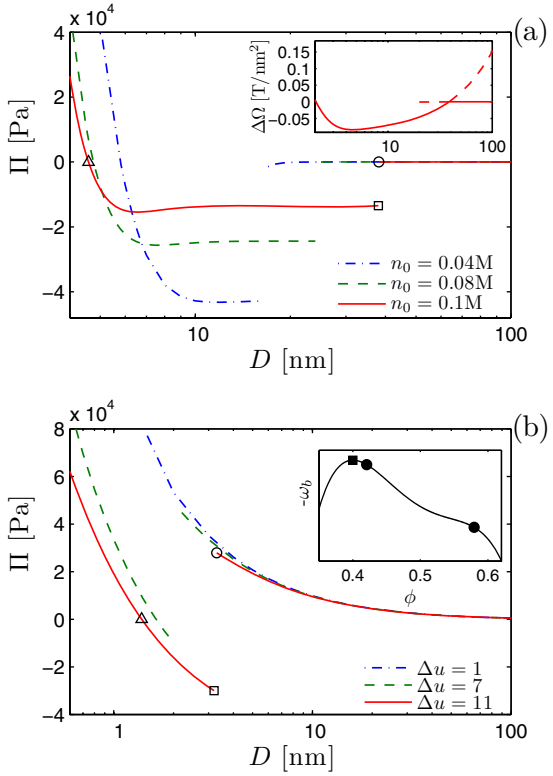

Fig. 2: (Colour on-line) (a) Osmotic pressure Π *vs.* surface separation D in the strong screening limit for different values of n_0 (other parameters as in fig. 1(a)). Inset: excess grand potential for $n_0 = 0.1\,\mathrm{M}$. solid (dashed) line corresponds to stable (metastable) solutions. (b) Π in the ideal gas regime for different values of Δu (other parameters as in fig. 1(b)). Inset: the function $-\omega_b(\phi)$. Filled square and circle markers correspond to ϕ_0 and the binodal compositions, respectively. In (a) and (b) open markers on solid lines correspond to distances D with the same symbols in fig. 1(a) and (b).

and is accompanied by a decrease in the osmotic pressure. This can lead to a negative osmotic pressure, such that a surface separation $D_e < D_t$ exists at which $\Pi = 0$. $\phi(z)$ at $D = D_e$ is shown by the dash-dot curves in fig. 1.

The excess grand potential per unit area relative to infinite separation is $\Delta\Omega(D) = -\int_\infty^D \Pi(D')\mathrm{d}D'$. $\Delta\Omega(D)$ has a cusp at $D = D_t$ and this results in a discontinuity of the pressure. Close to D_t, both a water-poor and a water-rich profiles are solutions of the Euler-Lagrange equations but only one of these is a stable solution. At $D > D_t$ the water-poor phase is stable, at $D < D_t$ the water-rich phase is stable, and at $D = D_t$ the grand potentials of the two phases are equal. Furthermore, $\Delta\Omega$ has a minimum at D_e ($D_e < D_t$) corresponding to mechanical equilibrium. An example of $\Delta\Omega(D)$ is shown in the inset of fig. 2(a), where the dashed line is $\Delta\Omega$ of metastable solutions.

The transition to a water-rich phase has a different physical origin in the two limiting cases. In the strong screening regime, the transition is promoted by the energy gained when the interface vanishes, as in capillary condensation. The thin water-rich layer near the walls remains nearly

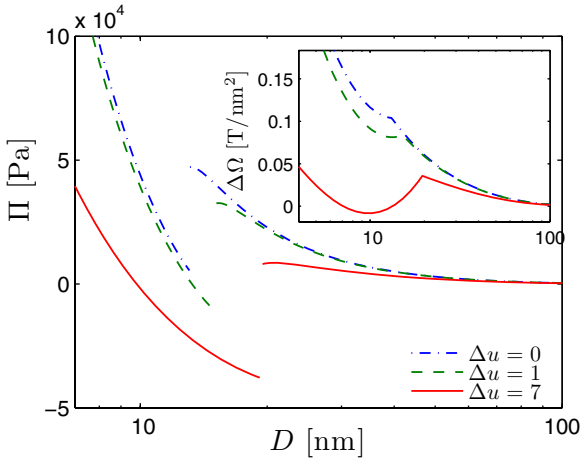

Fig. 3: (Colour on-line) Osmotic pressure in the weak screening regime with $n_0 = 10^{-4}\,\mathrm{M}$ and $\sigma = 1\,\mathrm{nm}^{-2}$ for three values of Δu. Inset: the corresponding excess grand potential $\Delta\Omega$.

independent of D. In the ideal gas regime, on the other hand, when the composition approaches the coexistence composition, preferential solvation promotes a transition to a water-rich phase. For intermediate cases, both mechanisms play a role in the transition. These effects are enhanced but are not limited to the vicinity of the critical temperature where the differences between the phases become smaller.

In fig. 2 we plot the osmotic pressure as a function of surface spacing; when $\Pi > 0$ the surfaces repel each other while for $\Pi < 0$ they attract. Π is discontinuous at $D = D_t$. In fig. 2(a) we show Π for different values of n_0 in the strong screening limit. An increase in n_0 decreases Π at large distances but increases it at small distances (entropy loss of the ions).

The negative jump in Π at $D = D_t$ increases with decreasing n_0. This can be explained by the interplay between the first two terms in eq. (6). At $D = D_t$ the increase in ϕ_m dominates the decrease in Π, an effect more pronounced for smaller values of n_0 since the positive ideal gas term is proportional to $n_m \propto n_0$. Recall that in a pure solvent only the ideal gas term exists and hence Π is always positive. Furthermore, this entropic repulsion will eventually dominate Π leading to $\Pi = 0$ at a separation D_e.

In fig. 2(b) we plot Π for different values of Δu in the ideal gas regime. For $\Delta u = 1$ the pressure is purely repulsive since preferential solvation is not strong enough to induce a water-rich phase. For $\Delta u = 7$ the interaction is repulsive down to D_t where Π becomes negative. When Δu increases to 11 the transition is at a larger distance and to a more negative pressure. The inset of fig. 2(b) shows the function $-\omega_b(\phi)$, showing a decrease in pressure at the transition (cf. eq (6)).

Figure 3 shows Π in the weak screening regime where $l_D \approx D$ and for three different values of Δu. When $\Delta u = 0$, the dielectrophoretic force alone can induce a water-rich

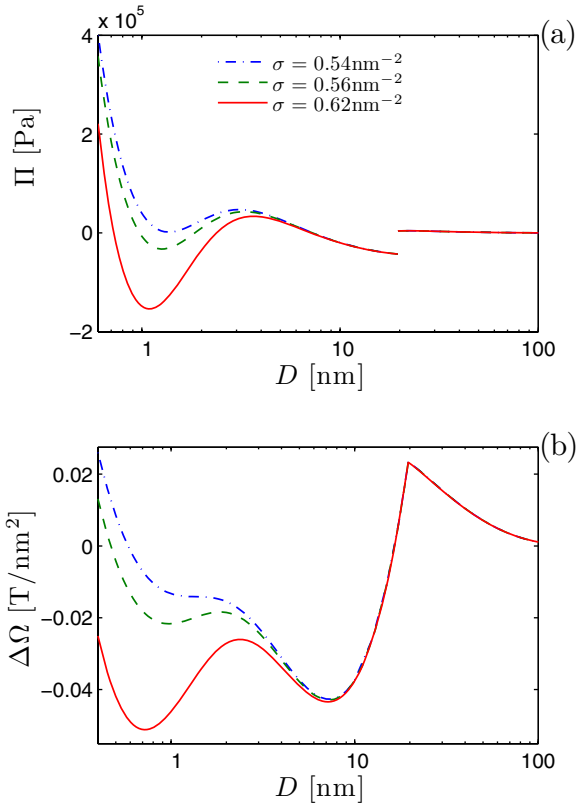

Fig. 4: (Colour on-line) (a) Osmotic pressure for $\Delta u = 10$, $n_0 = 10^{-4}$ M and three values of σ. (b) The corresponding excess grand potential. For $\sigma = 0.54\,\mathrm{nm}^{-2}$, $\Delta\Omega$ has only one minimum (dash-dot curve) at $D < D_t$. A second, metastable minimum appears for $\sigma = 0.56\,\mathrm{nm}^{-2}$ (dashed curve), whereas for $\sigma = 0.62\,\mathrm{nm}^{-2}$ (solid curve) this minimum becomes globally stable.

phase albeit the pressure is always repulsive [26]. The pressure can become attractive for $\Delta u = 1$ or 7. Corresponding curves of $\Delta\Omega$ are plotted in the inset of fig. 3. These show a metastable minimum at a finite value of D, $D = D_e$, for $\Delta u = 1$ and a global minimum for $\Delta u = 7$. The depth of the minimum for $\Delta u = 7$ is ≈ 440 T for two colloids with an effective surface area of $100\,\mathrm{nm} \times 100\,\mathrm{nm}$.

For $\Delta u = 10$, a second metastable minimum can appear in the curve $\Delta\Omega(D)$ at a smaller value of D, see the dashed and dash-dot curves in fig. 4. A similar value of Δu is cited in the literature for mixtures of water and 1-butanol containing NaCl at room temperature [12]. When σ is further increased (solid curves), this minimum can become globally stable. For large enough σ, only the second minimum exists (not shown). In this large Δu case, preferential solvation leads to the liquid between the surfaces being nearly pure water; ϕ_m is close to unity and ω_b diverges.

The distance D_t can be obtained in the two limiting cases presented in fig. 1. In the strong screening limit we use the continuity of $\Delta\Omega$ at D_t to obtain [27]

$$D_t \simeq 2t + 2\frac{\xi P_b + \int_{D/2-\xi-t}^{D/2-t} \omega(\phi(z))\mathrm{d}z}{P_b - P_h}. \qquad (7)$$

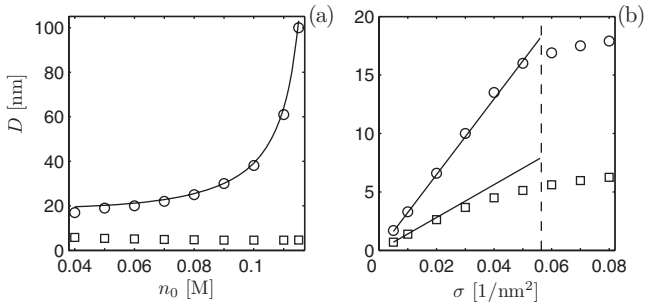

Fig. 5: Transition and equilibrium separations D_t (circles) and D_e (squares). (a) The strong screening case *vs.* n_0. (b) The ideal gas regime *vs.* σ. Solid curves are analytical expressions given in the text. In (a) we approximated $\phi(z)$ by a linear decrease from ϕ_h to ϕ_0 at the interface region. In (b), for σ beyond the dashed curve, a water-rich layer near the surfaces exists even as $D \to \infty$.

P_h, the pressure in the water-rich phase, is calculated at the midplane from $P_h = T(n_h^+ + n_h^-) - T\omega_b(\phi_h) + P_b$, where $n_h^\pm = n_0 \mathrm{e}^{\Delta u(\phi_h - \phi_0)}$ are the midplane values and ϕ_h is obtained from

$$\frac{\partial f_b}{\partial \phi}(\phi_h) - 2\Delta u n_0 \mathrm{e}^{\Delta u(\phi_h - \phi_0)} - \mu_0 = 0, \qquad (8)$$

where we used $\psi \approx 0$ at the midplane.

At $D = D_t$ the surfaces can be regarded as isolated and a zeroth-order approximation of ψ can be obtained using the well-known result for a single surface [1] with a homogeneous composition $\phi \approx \phi_h$ and a modified Debye length $(\varepsilon(\phi_h)T/(2e^2 n_0 \mathrm{e}^{\Delta u(\phi_h - \phi_0)}))^{1/2}$. Since at $|z| < D/2 - t$ $e\psi/T \ll \Delta u(\phi_h - \phi_0)$, t is obtained from the condition $e\psi/T = 0.01\Delta u(\phi_h - \phi_0)$. In analogy with classical mean field theory [24], the Landau expansion of eq. (8) around $\phi_c = 1/2$ gives for ξ

$$\xi \approx v_0^{1/3} \frac{1}{\sqrt{1 - \frac{T}{T_c} - 2\Delta u v_0 n_0 \mathrm{e}^{\Delta u(\frac{1}{2} - \phi_0)}\left(1 + \frac{\Delta u}{4}\right)}}. \qquad (9)$$

The preferential solvation term in the root is comparable in magnitude to $1 - T/T_c$. Thus, the bulk correlation length is modified appreciably by the preferential solvation of the ions.

Figure 5(a) shows the comparison of D_t from eq. (7) with numerical results for different values of n_0. The agreement is quite good despite the crude approximation. D_e in fig. 5(a) decreases slightly when n_0 increases, its value being ≈ 5 nm.

In the ideal gas regime $\phi(z) \approx$ const and the counterions density n^- is uniform and equal to the average charge density [24]: $\langle n^- \rangle \simeq 2\sigma/D$. The composition equation reads

$$\frac{\partial f_b}{\partial \phi} - \frac{2\Delta u \sigma}{D} - \mu_0 = 0. \qquad (10)$$

Here preferential solvation merely shifts the chemical potential of the mixture. Hence, D_t occurs when ϕ is the

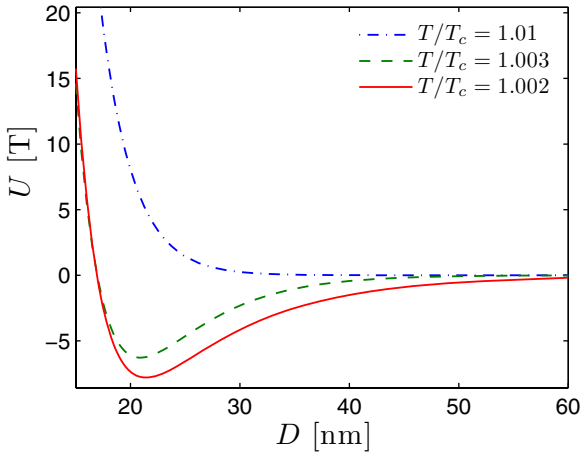

Fig. 6: (Colour on-line) Interaction potential $U = \Delta\Omega \times A$ for a mixture at a critical composition $\phi_0 = 1/2$ at three temperatures above T_c. For $T/T_c = 1.01$ (dash-dot curve) the interaction is purely repulsive. When the temperature is decreased the interaction turns attractive (dashed curve), becoming stronger closer to T_c (solid curve). Here $n_0 = 0.01\,\mathrm{M}$, $\Delta u = 4$ and $\sigma = 1\,\mathrm{nm}^{-2}$. The walls have a surface area of $A = 0.01\,\mu\mathrm{m}^2$.

binodal composition at which $\partial f_b/\partial\phi = 0$. Thus,

$$D_t \simeq -2\sigma\Delta u/\mu_0, \tag{11}$$

which means that $D_t \to \infty$ when the bulk composition approaches the binodal ($\mu_0 \to 0$).

D_e can be found by noting that $\Pi = 0$ in eq. (6) gives $n_e = \omega_b(\phi_e) + P_b/T$, where ϕ_e and n_e are the composition and ion density at D_e, respectively. Inserting this into eq. (4) we obtain for ϕ_e

$$\frac{\partial\omega_b}{\partial\phi}(\phi_e) = \Delta u\left(\omega_b(\phi_e) + P_b/T\right), \tag{12}$$

which is solved and then used to get n_e and D_e from the equations for Π and $\langle n^-\rangle$, respectively. Comparison of the formulae for D_t and D_e with the full numerical results are presented in fig. 5(b). As expected, the agreement is good for small values of σ where the ideal gas limit is valid. The dashed curve in fig. 5(b) marks the charge density above which a water-rich layer exists at infinite separation and the above approximations no longer hold.

We find that an attractive interaction is possible even at temperatures above T_c. Since at $T > T_c$ there is no miscibility gap, the first-order phase transition is missing and there is no discontinuity in the pressure. Instead, the pressure becomes smoothly attractive with decreasing plate distance. Figure 6 shows the interaction potential $U = \Delta\Omega \times A$ for two plates of surface A immersed in a critical mixture at three different temperatures. As the critical temperature is approached, a purely repulsive potential (dash-dot curve) becomes attractive (dashed curve). The interaction is more attractive closer to T_c (solid curve). The depth and location of the minimum in the curves and their dependence on the temperature are similar to those observed in recent experiments on the salt-dependent interaction of a charged particle suspended in a critical binary mixture near a charged wall [21]. Thus, the mechanism we describe may be important to capture correctly electrostatic effects in these experiments. We believe that it is possible to attribute some of the results of these experiments to a solvation related force [28] in addition to the critical Casimir force.

The qualitative difference in the interaction between charged colloids or macromolecules in mixtures compared to pure solvents stems from the contribution to Π of the second term in eq. (6): $\omega_b(\phi_m)$ – the midplane mixture grand potential. This term is absent in pure solvents. Thus, unlike similar ion-induced phase transitions in pure solvents [29] we observe a jump to a *negative* pressure (at $D_t \approx 1$–$100\,\mathrm{nm}$). Moreover, the nontrivial dependence of $\omega_b(\phi_m)$ on the system parameters (T,ϕ_0,n_0,σ) through the governing equations leads to qualitatively different behavior compared to usual condensation transitions due to surface fields [27]. In addition, the attractive force is in many cases strong and long-range compared to the van der Waals force [1] as is evident by the values of Π at $D = D_t$ (fig. 2 and fig. 3) and the energy minimum being deeper than $\sim 100\,\mathrm{T}$.

The mechanism we describe should be at play in the aggregation of charged colloids in mixtures near the coexistence temperature [18,19]. We believe it is directly relevant to the attraction seen between colloids and surfaces in critical mixtures and attributed to the critical Casimir force [20–22].

* * *

We gratefully acknowledge numerous discussions with D. Andelman, C. Bechinger, M. Bier, H. Diamant, J. Dietrich, S. Dietrich, L. Helden, O. Nelen, A. Onuki, P. Pincus, R. Podgornik, S. Safran, M. Schick, and T. Witten. This work was supported by the Israel Science Foundation under grant No. 11/10 and the European Research Council "Starting Grant" No. 259205.

REFERENCES

[1] Israelachvili J. N., *Intermolecular and Surface Forces,* 2nd edition (Academic Press, London) 1992.
[2] Kjellander R. and Marčelja S., *Chem. Phys. Lett.*, **127** (1986) 402.
[3] Lau A. W. C., Levine D. and Pincus P., *Phys. Rev. Lett.*, **84** (2000) 4116.
[4] Burak Y. and Andelman D., *Phys. Rev. E*, **62** (2000) 5296.
[5] Moreira A. G. and Netz R. R., *Europhys. Lett.*, **52** (2000) 705.
[6] Naji A., Kanduč M., Netz R. R. and Podgornik R., *Exotic electrostatics: Unusual features of electrostatic*

interactions between macroions, in *Understanding Soft Condensed Matter via Modeling and Computation*, edited by Hu W.-B. and Shi A.-C. (World Scientific, Singapore) 2010.
[7] Netz R., *Eur. Phys. J. E*, **5** (2001) 557.
[8] Moreira A. G. and Netz R. R., *Phys. Rev. Lett.*, **87** (2001) 078301.
[9] Marcus Y., *J. Chem. Soc., Faraday Trans. 1*, **84** (1988) 1465.
[10] Osakai T. and Ebina K., *J. Phys. Chem. B*, **102** (1998) 5691.
[11] Hung L. Q., *J. Electroanal. Chem.*, **115** (1980) 159; **149** (1983) 1.
[12] Marcus Y., *Pure Appl. Chem.*, **55** (1983) 977.
[13] Ben-Yaakov D., Andelman D., Podgornik R. and Harries D., to be published in *Curr. Opin. Colloid Interface Sci.* (2011) doi:10.1016/j.cocis.2011.04.012.
[14] Onuki A., *Phys. Rev. E*, **73** (2006) 021506.
[15] Okamoto R. and Onuki A., *Phys. Rev. E*, **82** (2010) 051501.
[16] Onuki A., *J. Chem. Phys.*, **128** (2008) 224704.
[17] Ben-Yaakov D., Andelman D., Harries D. and Podgornik R., *J. Phys. Chem. B*, **113** (2009) 6001.
[18] Beysens D. and Estève D., *Phys. Rev. Lett.*, **54** (1985) 2123.
[19] Law B. M., Petit J.-M. and Beysens D., *Phys. Rev. E*, **57** (1998) 5782.
[20] Hertlein C., Helden L., Gambassi A., Dietrich S. and Bechinger C., *Nature*, **451** (2008) 172.
[21] Nellen U., Dietrich J., Helden L., Chodankar S., Nygrd K., van der Veen J. F. and Bechinger C., *Soft Matter*, **7** (2011) 5360.
[22] Bonn D., Otwinowski J., Sacanna S., Guo H., Wegdam G. and Schall P., *Phys. Rev. Lett.*, **103** (2009) 156101.
[23] Tsori Y. and Leibler L., *Proc. Natl. Acad. Sci. U.S.A.*, **104** (2007) 7348.
[24] Safran S., *Statistical Thermodynamics of Surfaces Interfaces, and Membranes* (Westview Press, New York) 1994.
[25] Landau L. D., Lifshitz E. M. and Pitaevskii L. P., *Electrodynamics of Continuous Media,* 2nd edition (Butterworth-Heinemann, Amsterdam) 1984.
[26] Tsori Y., Tournilhac F. and Leibler L., *Nature*, **430** (2004) 544.
[27] Evans R., Marconi U. M. B. and Tarazona P., *J. Chem. Phys.*, **84** (1986) 2376.
[28] Bier M., Gambassi A., Oettel M. and Dietrich S., arXiv:1104.5703v1, (2011).
[29] Harries D., Podgornik R., Parsegian V. A., Mar-Or E. and Andelman D., *J. Chem. Phys.*, **124** (2006) 224702.